Bulletin of the Seismological Society of America, Vol. 98, No. 2, pp. 692–708, April 2008, doi: 10.1785/0120070021

The Attenuation of Seismic Intensity in Italy, Part II: Modeling and Validation

by C. Pasolini, D. Albarello, P. Gasperini, V. D'Amico,* and B. Lolli

Abstract Several different attenuation models have recently been proposed for the Italian region to characterize the decay of macroseismic intensity with the distance from the source. The significant scatter between these relationships and some significant drawbacks that seem to characterize previous approaches (described in a companion article by Pasolini *et al.*, 2008) suggest that the problem needs to be reconsidered. As a first step toward more detailed analyses in the future, this study aimed at developing an isotropic attenuation relationship for the Italian area. Because this attenuation relationship has to be used primarily in probabilistic seismic hazard assessment, major attention was given to evaluating the attenuation relationship in its complete probabilistic form. Another important aspect of this study was the preliminary evaluation of the intrinsic (i.e., independent of the specific attenuation relationship to be used) scattering of data, which represents the lowest threshold for the residual variance that cannot be explained by the attenuation relationship. Furthermore, the peculiar formal features of intensity data and relevant uncertainties were considered carefully. To reduce possible biases, the completeness of the available database was checked and a suitable data selection procedure was applied. Since epicentral intensity cannot be defined unambiguously from the experimental point of view, the attenuation relationship was scaled with a new variable that is more representative of the earthquake dimension. Several criteria were considered when evaluating competing attenuation formulas (explained variance, Bayesian information criteria, Akaike information criteria, etc.). Statistical uncertainty about empirical parameters was evaluated by using standard approaches and bootstrap simulations. The performance of the selected relationship with respect to a control sample was analyzed by using a distribution-free approach. The resulting equation for the expected intensity I at a site located at epicentral distance R is

$$I = I_E - (0.0086 \pm 0.0005)(D - h) - (1.037 \pm 0.027)[\ln(D) - \ln(h)],$$

where $D = \sqrt{R^2 + h^2}$, $h = (3.91 \pm 0.27)$ km, and I_E is the average expected intensity at the epicenter for a given earthquake that can be computed from the intensity data (when available) or by using empirical relationships with the moment magnitude M_w or the epicentral intensity I_0 reported by the Italian seismic catalog

$$I_E = -(5.862 \pm 0.301) + (2.460 \pm 0.055)M_w,$$
$$I_E = -(0.893 \pm 0.254) + (1.118 \pm 0.033)I_0.$$

Comparison of the model standard deviation (S.D.) (0.69 intensity degrees) with the intrinsic one (0.62) indicates that this attenuation equation is not far from being optimal.

*Present address: Istituto Nazionale di Geofisica e Vulcanologia, Via della Faggiola, 32, I-56126 Pisa, Italy; damico@pi.ingv.it.

Introduction

The macroseismic intensity scale, despite its apparent aging, continues to be an important tool in modern seismology, particularly in the assessment of seismic hazards. In fact, more than 60% of national hazard maps worldwide are expressed in terms of macroseismic intensity (McGuire, 1993). Furthermore, this parameter appears to be irreplaceable for the representing of damage scenarios for possible future earthquakes. Because of the relatively low seismicity rate, in many countries (such as Italy), most of the information about major past earthquakes comes from documentary sources that date back to the preinstrumental age (e.g., for more than 70% of major Italian earthquakes, only noninstrumental data are available). This being so, it is only in terms of macroseismic information that the parameterization of such events can be achieved. The nature of the available information also justifies the significant present-day research activity in the field of macroseismics, even in other countries (e.g., Musson, 2005; Bakun, 2006; Bakun and Scotti, 2006).

In the context of a general reassessment of hazard maps of Italy, a number of recent articles (Gasperini, 2001; Carletti and Gasperini, 2003; Albarello and D'Amico, 2004; Rotondi and Zonno, 2004; Azzaro *et al.*, 2006) have, using different approaches and perspectives, reassessed the empirical relationships regarding the attenuation of intensity with distance. These different approaches and perspectives have resulted in a number of different attenuation relationships being posited for the same area. The discrepancies among such relationships prompted us to reexamine the issue of determining the attenuation relationships, with a particular focus on examining and reconciling the different competing views present in the literature. Thus, in a companion article (Pasolini *et al.*, 2008) some of the attenuation relationships cited here have been critically reanalyzed. The analysis shows that most of the discrepancies between the obtained results are the consequence of different views of the problem and of hidden assumptions. In fact, some of these assumptions are probably wrong and might bias the predictive ability of the relevant attenuation relationships. In particular, Pasolini *et al.*, showed that (1) intensity observations at relatively large epicentral (hypocentral) distances, where expected effects are below the limit of diffuse perceptibility (about degree IV), are incomplete; thus, attenuation relations obtained by considering these data tend to overestimate intensity at large distances, and (2) epicentral intensities reported in the Italian catalog are not consistent with the intensity predicted at the epicenter by attenuation relations.

Our first aim in the present article is to clarify our goal and strategy with respect to the empirical assessment of attenuation relationships. The main objective is to develop the attenuation relationship in the complete probabilistic form (see, e.g., Albarello and D'Amico, 2005), which is the one required by numerical codes that are devoted to the probabilistic assessment of seismic hazard (e.g., Bender and Perkins, 1987). That is,

$$\text{prob}[I \geq I_s | J, D] = 1 - P(I_s | J, D), \tag{1}$$

where P is the probability distribution, I_s is the intensity at the site s, and D and J are functions of the distance of the site from the source and the energy released at the source, respectively.

Particular attention has been paid to characterizing the variance associated with the considered probability distribution, because this factor affects hazard estimates dramatically (Cornell, 1971; Brillinger, 1982; Albarello and D'Amico, 2004). In this study, the peculiar role of uncertain intensity values (e.g., III–IV) has been considered explicitly.

In order to maximize the informative content of the available data set, we restricted our analysis to one isotropic relationship for the whole Italian area. This might represent the first step towards more sophisticated approaches (e.g., Carletti and Gasperini, 2003).

After describing the selected data set briefly, we discuss the form of the attenuation relationship along with the relevant parameters. Thus, we analyze and apply statistical criteria to parameterize and validate empirical attenuation relationships.

The Data Set

Seismic Compilations

The data set used for the analysis consists of the most recent version of the Parametric Catalog of Italian Earthquakes (CPTI04) (CPTI Working Group, 2004) and the related database of macroseismic intensity observations in Italy (DBMI04) (DBMI Working Group, 2007). These databases were constructed by combining and elaborating upon previous macroseismic data collections (Boschi *et al.*, 1995, 1997, 2000; Monachesi and Stucchi, 1997). The CPTI04 catalog contains epicentral information for 2551 damaging (or potentially damaging) earthquakes that have occurred in Italy since 217 B.C. For 1042 of them, the DBMI04 macroseismic database reports a collection of intensity estimates at different localities (macroseismic field) based on documentary information. For most of the remaining earthquakes, the parametrization is also based on mainly macroseismic information, but documentation on effects at individual sites is lacking (no associated macroseismic field is available). For earthquakes provided with a macroseismic field, the reported epicenter is computed as the barycenter of the localities at which the highest intensities were observed, according to the procedure described by Gasperini *et al.* (1999) and Gasperini and Ferrari (2000). Such an algorithm, using a robust estimator (trimmed mean), has proven to be fairly stable with respect to site misplacement and errors regarding the assessment of intensity. For these earthquakes, the catalog also reports the epicentral intensity I_0. This value is computed according to another algorithm, also described by Gasperini *et al.* (1999) and Gasperini and Ferrari (2000). Generally, I_0

corresponds to the highest intensity observed for the relevant earthquakes. In cases in which local site amplification is likely to have occurred, this maximum intensity has been suitably reduced. In a few cases, the epicentral intensity has been manually adjusted to take into account specific situations (e.g., epicenter located offshore).

In all, the macroseismic database includes 58,926 macroseismic observations made at 14,821 different sites. Some of these sites (about 100) are not associated with a well-defined location but refer to very rough geographical definitions (e.g., northern Italy). These sites cannot be considered in the analysis. About 10,000 macroseismic observations are not expressed in terms of standard intensity values (e.g., felt, damages) defined by the Mercalli–Cancani–Sieberg (MCS) scale (Sieberg, 1931). Therefore, only about 48,000 observations are suitable for use in the statistical analysis of intensity attenuation.

Data Selection

Epicentral parameters based on few intensity data can be biased by the uneven spatial distribution of observing sites and by local amplification effects. Hence, we only consider earthquakes the intensities of which are documented at a minimum of 10 different sites. We also excluded the data for earthquakes that occurred before A.D. 1200 and all intensity estimates that were deduced from the effects on single edifices rather than on settlements.

A careful screening of earthquakes located near the sea coast has also been carried out. Actually, in these cases, the asymmetric distribution of observations might induce a drift of the possible off-shore epicenter toward the coast and a bias of the relevant attenuation pattern. To detect earthquakes whose epicentral location was possibly biased in this way, we considered, for all of the events located close to the coastline, the intensity attenuation pattern as well as the aspect ratio of the area that showed the largest effects: narrow areas along the coast are assumed to indicate an off-shore epicenter, while almost circular ones have been associated with an epicenter located inland. Fortunately, there are few off-shore seismogenic sources in Italy that show significant activity. Table 1 reports 30 earthquakes that are not used in this study because their true epicenters are likely to be located offshore.

We also excluded the earthquakes that occurred at the volcanic areas of Mt. Etna and Ischia island. Both areas are known to be strongly attenuating, due to their volcanic nature (see Carletti and Gasperini, 2003; Azzaro *et al.*, 2006). In particular, we excluded from the database two events that occurred at Ischia island in 1881 and 1883, as well as all earthquakes located within a radius of 25 km from the summit of Mt. Etna (latitude 37.73, longitude 15.00). The application of all these selection criteria further reduces the number of earthquakes to about 470 and the number of intensity data that are used in computations to 39,000.

Completeness of Macroseismic Data Sets

As discussed in the companion article (Pasolini *et al.*, 2008) intensity values of less than degree IV MCS are observed by few or very few people, and thus it is possible they are not included in macroseismic reports about small settlements. This incompleteness actually results in an apparent reduction of intensity attenuation at relatively long distances from the source (>100 km) and represents one of the main causes of the predictive inadequacy of some previous analyses (Pasolini *et al.*, 2008). This bias can be removed by adopting the procedure originally proposed by Gasperini (2001), which consists of excluding all intensities observed at a distance greater than that at which an intensity below IV is expected on the basis of a preliminary attenuation relationship. This selection criterion does not introduce a further bias because it applies to hypocentral distances and not to observed intensities. Thus, the procedure for selecting data proposed by Gasperini (2001) and reported explicitly by Pasolini *et al.* (2008) has been adopted here. As result, the data set of usable intensities is reduced further, to about 22,500 documented intensity values.

Statistical Formalization

Uncertain Intensity Values

A significant portion (about 30%) of the intensity data that remained after following the procedure for selection described above corresponds to uncertain intensity assessments (e.g., VII–VIII). These are often reported in the form of a decimal value (e.g., 7.5). These intensity estimates have to be interpreted as meaning that (1) the lower degree (e.g., VII) has certainly been reached at the site, but (2) there is also evidence (perhaps weak) that the higher value (e.g., VIII) is possible but not certain. There are several ways to consider such data. For example, Gasperini (2001) used them as real intensity values positioned in the middle of the interval between the two degrees. Albarello and D'Amico (2004, 2005) assumed instead that both the contiguous integer values (VII and VIII MCS) are equally possible outcomes (see also Grünthal, 1998) but used this assumption only to validate the attenuation relation and discarded all uncertain data for the fit of the attenuation equation. Magri *et al.* (1994) proposed to assign to each intensity degree of the considered macroseismic scale a degree of belief expressed in terms of probability $p(I)$). When using this approach, writing VII–VIII corresponds to a probability density distribution in the form

$$p(I) \equiv [0, 0, 0, 0, 0, 0, 0, w_1, w_2, 0, 0, 0, 0], \tag{2}$$

with the condition that

$$\sum_I p(I) = 1. \tag{3}$$

Table 1

Earthquakes Excluded from Computation Because the Epicenter Is Known or Is Supposed to Be Located in the Sea

Year	Month	Day	Hour	Minute	Second	Latitude	Longitude	Epicentral Area	Data	I_0
1690	12	23	0	20		43.546	13.593	Ancona area	17	8.0
1743	2	20	16	30		39.852	18.777	Southern Ionian sea	77	9.0
1823	3	5	16	37		37.993	14.094	Northern Sicily	107	8.0
1831	5	26	10	30		43.855	7.849	Western Liguria	33	8.0
1848	1	11				37.543	15.174	Augusta	41	7.5
1854	12	29	1	45		43.813	7.543	Western Liguria–France	86	7.5
1875	3	17	23	51		44.062	12.547	Southeastern Romagna	144	8.0
1882	8	16				42.979	13.875	Grottammare	13	7.0
1887	2	23	5	21	50	43.891	7.992	Western Liguria	1517	9.0
1889	12	8				41.830	15.692	Apricena	122	7.0
1896	10	16				43.909	7.872	Albenga	60	6.0
1905	9	8	1	43	11	38.670	16.068	Calabria	827	10.0
1916	5	17	12	50		44.010	12.623	Northern Adriatic sea	132	8.0
1916	8	16	7	6	14	43.961	12.671	Northern Adriatic sea	257	8.0
1917	11	5	22	47		43.506	13.586	Numana	26	6.0
1919	10	22	6	10		41.462	12.637	Anzio	138	6.5
1924	1	2	8	55	13	43.736	13.141	Central Adriatic sea	76	7.5
1926	8	17	1	42		38.567	14.825	Salina island	44	7.0
1930	10	30	7	13		43.659	13.331	Senigallia	263	8.0
1972	1	18	23	26		44.203	8.163	Western Ligurian coast	41	6.0
1972	1	25	20	25	11	43.614	13.355	Central Adriatic sea	24	6.0
1972	2	4	2	42	53	43.590	13.295	Central Adriatic sea	75	7.5
1972	2	4	9	19	4	43.589	13.283	Central Adriatic sea	56	7.5
1972	2	29	20	54		41.841	15.459	Southern Adriatic sea	21	6.0
1972	6	14	18	55	46	43.580	13.416	Central Adriatic sea	17	8.0
1978	4	15	23	33	47	38.125	15.022	Gulf of Patti	333	8.0
1982	3	21	9	44	2	40.008	15.766	Gulf of Policastro	126	7.5
1984	4	22	17	39	21	43.617	10.313	Leghorn	39	6.0
1990	12	13	0	24	28	37.266	15.121	Southeastern Sicily	304	7.0
2002	9	6	1	21	29	38.081	13.422	Palermo	132	6.0

We adopted this representation, and we also assumed initially, as did Albarello and D'Amico (2005), that $w_1 = w_2 = 0.5$. However, this latter assumption is, to some extent, arbitrary and needs to be tested against different choices. This representation can also be applied to well-defined integer intensity values. In the latter case, the probability vector is 1 for the corresponding degree and 0 for all of the others. Note that this probabilistic approach implies an appropriate statistical treatment for the empirical parameterization of attenuation.

Log-Likelihood Approach

A likelihood approach has been adopted to find the best-fit parameters for the different attenuation relationships. This approach allows the presence of ill-defined intensity data (see previous section) to be taken into account and also makes it easier to fit nonlinear relationships.

The likelihood function of a set of N observations (the total probability that they represent a realization of a given stochastic process) can be written as the product of their independent probabilities:

$$\ell = \prod_{j=1}^{N} g_j(\boldsymbol{\theta}), \tag{4}$$

where g_j is the probability of the jth observation, and $\boldsymbol{\theta}$ is the set of model parameters.

When (as in the case of intensity) some observations are uncertain in the sense described here, we have to compute $g_j(\boldsymbol{\theta})$ by the total probability theorem:

$$g_j(\boldsymbol{\theta}) = \sum_{I=1}^{12} p_j(I) g_j(\boldsymbol{\theta}|I), \tag{5}$$

where $g_j(\boldsymbol{\theta}|I)$ is the probability of the jth observation, given that the intensity I actually occurred. In this case, the likelihood function (4) becomes

$$\ell = \prod_{j=1}^{N} \left[\sum_{I=1}^{12} p_j(I) g_j(\boldsymbol{\theta}|I) \right]. \tag{6}$$

As intensity is discrete in nature, the application of a continuous distribution model (such as the Normal one) must take into account this peculiarity. Thus, the total probability of a given integer observation I must be computed as the integral of the probability density function over the interval of the continuous variable $[I-0.5, I+0.5]$ that the integer observation represents:

$$g_j(\boldsymbol{\theta}|I) = \int_{I-0.5}^{I+0.5} h_j(\boldsymbol{\theta}, i)\, di, \tag{7}$$

where $h(\boldsymbol{\theta}, i)$ is the probability density function of the statistical distribution used to represent attenuation.

Gasperini (2001) and Albarello and D'Amico (2004) showed that the distribution of intensity residuals for the Italian data set is close to Normal. Thus, such a distribution can be assumed under the hypothesis that the discrepancies from normality, albeit statistically significant, are not relevant in practice for the evaluation of attenuation parameters. In this case, equation (7) becomes

$$g_j(\boldsymbol{\theta}|I) = \frac{1}{\sigma\sqrt{2\pi}} \int_{I-0.5}^{I+0.5} \exp\left[-\frac{(i-\mu_j)^2}{2\sigma^2}\right] di, \tag{8}$$

where μ_j is the expectation relative to the jth observation (that is a function of model parameters), and σ is the relevant S.D..

Substituting equation (8) in (6) and taking the logarithm gives the log-likelihood function that can be maximized numerically to find the best-fitting parameters of the model:

$$L = \sum_{j=1}^{N} \ln\left\{\frac{1}{\sigma\sqrt{2\pi}} \sum_{I=1}^{12} p_j(I) \int_{I-0.5}^{I+0.5} \exp\left[-\frac{(i-\mu_j)^2}{2\sigma^2}\right] di\right\}. \tag{9}$$

For maximizing L, we tested some optimization codes based on simulated annealing (Metropolis and Ulam, 1949; Goffe *et al.*, 1994) and genetic algorithms (Holland, 1975; Goldberg, 1989; Carrol, 1996). However, we have verified that, due to the fact that the likelihood function as a function of unknown parameters is reasonably regular, reliable results can be obtained using the faster and more accurate quasi-Newton method (Dennis and Schnabel, 1983) implemented by the Fortran routine DUMINF of the International Mathematics and Statistics Library (IMSL) (Visual Numerics, 1997).

The Intrinsic Variability of the Data Set

Intensities vary mainly with the distance from the source and the strength of the source. However, further variations can be induced by a number of additional factors, such as near-source radiation pattern, local amplification of seismic motion induced by the local stratigraphy and topography, and regional differences in the energy propagation pattern (Carletti and Gasperini, 2003). The presence of such further factors of variations implies that, whatever isotropic attenuation model we introduce, part of the variability in intensity will remain unexplained, and a lower bound will exist for the model variance. Since this variance does not depend on the specific attenuation model considered, we named it intrinsic variability.

To estimate such intrinsic variability, we grouped intensity observations relative to each mth earthquake in contiguous 5-km bins of epicentral distance. For each bin, we computed the S.D. σ_l^m of the relevant intensities with respect to the average intensity μ_l^m in each lth bin. To be consistent with our likelihood formulation, σ_l^m and μ_l^m are computed by maximizing equation (9), where σ_l^m and μ_l^m take the place of σ and μ_j, respectively. Only bins characterized by at least 10 observations were considered. The intrinsic S.D. relative to each distance bin for the entire intensity database was computed as

$$\sigma_l^{\text{intr}} = \sqrt{\frac{\sum_{m=1}^{N_l} (\sigma_l^m)^2 M_l^m}{\sum_{m=1}^{N_l} M_l^m}}, \tag{10}$$

where M_l^m is the number of intensity observations in the lth-distance bin for the mth earthquake, and N_l is the number of earthquakes with at least 10 observations in the lth-distance bin.

The results of these computations (reported in Fig. 1) indicate that the intrinsic S.D. is nearly constant (homoscedastic) up to about 140 km from the source and equal to about 0.62 intensity degrees. The absence of a clear trend at longer distances reasonably supports the assumption of homoscedasticity over the whole distance range. It is worth noting that such a value for the S.D. is much lower than those relative to empirical intensity relationships so far computed, which in all cases are greater than 1.0 (Gasperini, 2001; Albarello and D'Amico, 2004). This difference indicates that such models are far from optimal for representing intensity attenuation in Italy.

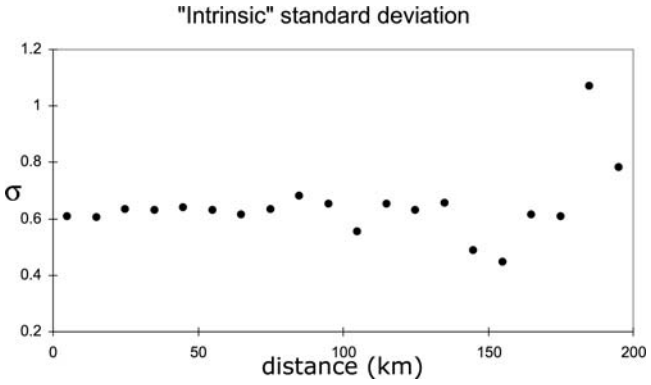

Figure 1. Standard deviation of observed intensities in each distance bin (see text for details).

The Attenuation Model

Although a physical theory of seismic intensity is obviously not available, there is much evidence to support its proportionality with the logarithm of ground motion amplitude (see also the discussion in Pasolini *et al.*, 2008). Here, we generally adopt this hypothesis; hence, we assume at first that the expectation μ to be used in equation (9) is described by a relationship similar to the one used in most ground motion attenuation relationships developed for engineering purposes. In particular, we adopted the form

$$\mu(J, D) = J + a(D - D_0) + b \ln\left(\frac{D}{D_0}\right), \qquad (11)$$

where D is some expression of the distance from the source, D_0 is an arbitrary reference distance, and J is the excitation term (also depending on the choice of D_0) that represents any empirical equivalent, in terms of intensity, of the source strength. The coefficients a and b quantify anelastic (and/or scattering) dissipation and geometrical spreading, respectively. We must note that equation (11) implies the assumption that the reduction of intensity with distance is independent of the excitation term.

The assumption of a Gaussian distribution (see the section entitled Statistical Formalization) implies that the attenuation relationship in its complete probabilistic form (1) will be

$$F(I_s) = \text{prob}[I \geq I_s | J, D] = \frac{1}{\sigma\sqrt{2\pi}} \int_{I_s - 0.5}^{\infty} e^{-\{[i-\mu(J,D)]^2/2\sigma^2\}}\, di. \qquad (12)$$

Note that, being just a parameter of the probability distribution (12), the value of the expectation $\mu(J, D)$ is not an actual intensity value and thus it can assume any real value. Because of the findings detailed in the section entitled The Intrinsic Variability of the Data Set, σ is assumed to be independent of D. In addition, we assume that σ is also independent of J.

All the parameters in (11) have to be determined empirically by the statistical analysis of available data. Of course, several alternative formulations are possible (von Kővesligethy, 1906; Blake, 1941; Howell and Schultz, 1975; Gupta and Nuttli, 1976; Chandra, 1979; Chandra *et al.*, 1979; Tilford *et al.*, 1985; Berardi *et al.*, 1993; Peruzza, 1996; Gasperini, 2001; Lee and Kim, 2002), some of which will be considered later in the discussion. However, we have chosen equation (11) for its obvious physical justification, as well as for its widespread usage by most of investigators.

At first, the discussion will concentrate on the two independent variables D and J.

The Parameter D

D can be defined in several ways. The simplest one considers the distance R between the macroseismic epicenter and the site. This, however, neglects the evidence that seismic waves come mainly from the depth at which the earthquake rupture occurs. Moreover, the logarithmic term becomes singular when intensity values at the epicenter are considered. Thus, it is a common practice to compute D as a sort of hypocentral distance in the form

$$D = \sqrt{R^2 + h^2}, \qquad (13)$$

where h represents an empirical equivalent of the hypocentral depth (e.g., von Kővesligethy, 1906; Blake, 1941). Although rough (because it does not correspond to the actual length of the path of the seismic waves in the Earth), this approximation is certainly more realistic than assuming that waves radiate from the epicenter. Previous approaches (e.g., Gasperini, 2001; Albarello and D'Amico, 2004) have assumed a fixed source depth ($h = 10$ km) on the basis of a rough empirical evaluation of the average depth distribution of Italian instrumental hypocenters. However, because the hypocentral depth might differ significantly from the centroid of seismic energy radiation, in principle one could obtain a better estimate of source depth from the data themselves. This could be done by allowing h to vary independently for each earthquake and by determining its value from a statistical analysis. However, this would imply a strong increase in the number of free parameters to be determined. Since a strong interplay among free parameters is expected, any additional parameter could reduce stability of final results. Thus, we decided to assume a common depth for all earthquakes, which may be viewed as the average depth of the apparent radiating source.

Another issue concerns the possible bias induced, particularly for strong earthquakes, by the finite source extension at short epicentral distances. In fact, the assumption of spherical (or cylindrical) symmetry of wave propagation from the hypocenter is rather crude for seismic sources of magnitude larger than 5 associated with fault lengths larger than 5 km (Wells and Coppersmith, 1994). The assumption of circular symmetry, when the source dimension is not negligible, generally overestimates the actual distance from the source to the sites along the fault trace. The Joyner–Boore distance (the closest distance from a site to the surface projection of the fault) is sometimes adopted to correct this bias in peak ground acceleration (PGA) attenuation studies (Ambraseys *et al.*, 1996; Sabetta and Pugliese, 1996). However, the Joyner–Boore distance cannot be applied easily to historical earthquakes due to the general lack of information about the relevant source geometry.

Gasperini (2001) and Albarello and D'Amico (2004) addressed this problem by discarding intensity data that are closer to the source than a minimum threshold $D_{\min} = \sqrt{R^2_{\min} + h^2}$. Gasperini (2001) computes $D_{\min}$ as a function

of the macroseismic moment magnitude, while Albarello and D'Amico (2004) assume $D_{\min} = 15$ km for all earthquakes. Although the method by Gasperini (2001) might appear more accurate, it could bias the analysis because it selects the data points as a function of earthquake magnitude. As a result, only the data coming from small earthquakes would be selected at short distances, and thus the estimated attenuation properties in this range of distances would only reflect the attenuation behavior for such earthquakes. On the other hand, the assumption of a fixed threshold results in near-source data being discarded completely, yet the prediction of intensity in the vicinity of the sources is crucial in hazard assessment.

On the basis of these considerations, we decided to assume initially that $R_{\min} = 0$ (i.e., no data are discarded). We will discuss the effects of applying different thresholds in the section entitled Discussion and Validation of Regression Results.

The Parameter J

The formula (13) for hypocentral distance suggests that a convenient choice is to set $D_0 = h$ in equation (11) so that the expectation becomes

$$\mu(J, D) = J + a(D - h) + b \ln\left(\frac{D}{h}\right). \qquad (14)$$

J then corresponds to the intensity expected at the epicenter ($\mu(J, h) = J$) on the basis of the attenuation model considered. To best underline the epicentral nature of J in what follows, we will use the symbol I_E (also used with a similar meaning by Pasolini *et al.*, 2008) in place of J.

The most natural estimators of I_E are the maximum observed intensity $I_{\max}$ or epicentral intensity I_0, which are usually available for any macroseismically observed earthquake. However, one of the disadvantages of these estimators is their sensitivity to possible local conditions responsible for site effects. Furthermore, Pasolini *et al.* (2008) showed that the values of I_0 and $I_{\max}$ reported in the Italian seismic catalogs are generally inconsistent with attenuation relationships so far proposed.

A possible alternative approach, similar to the procedure proposed by Pasolini *et al.* (2008), is to determine I_E values consistently with the attenuation model. To adopt this approach, we perform the analysis in two steps described in the next section.

Two-Step Regression Procedure

In order to use attenuation relationships (equation 14) in seismic hazard computations, the values of four free parameters (a, b, h, σ) have to be estimated from the whole data set, along with consistent values of the source term I_E relative to each earthquake. A two-step regression analysis was adopted to reduce the trade-off between propagation and source terms and to account consistently for the uncertainties relative to the source term, which are not negligible. In the first step, the parameters representative of the distance dependence are determined independently of the source term I_E. In the second step, the latter term is determined from the results of the previous step or from other information.

First Step

We can eliminate I_E from equation (14) by considering first an empirical average $\bar{I}_m$ of the observed intensities relative to each mth earthquake and located within a given epicentral distance $R_{\max}$. Then $\bar{I}_m$ can reasonably be forced to coincide with the arithmetic average of expectations given by equation (14) (where I_E substitutes J). This corresponds to

$$\bar{I}_m \equiv I_E + a\frac{1}{M_m}\sum_{k=1}^{M_m} D_k^m - ah + b\frac{1}{M_m}\sum_{k=1}^{M_m}\ln(D_k^m) - b\ln(h), \qquad (15)$$

where M_m is the number of available observations for the mth events at distances shorter than $R_{\max}$. Then, subtracting (15) from (14), we get

$$\mu(\bar{I}_m, D) = \bar{I}_m + a(D - \bar{D}_m) + b[\ln(D) - \overline{\ln(D)_m}], \qquad (16)$$

where

$$\bar{D}_m = \frac{1}{M_m}\sum_{k=1}^{M_m} D_k^m; \qquad \overline{\ln(D)}_m = \frac{1}{M_m}\sum_{k=1}^{M_m}\ln(D_k^m). \qquad (17)$$

Note that equation (16) is independent of I_E and thus can be used to empirically fit the distance dependence without considering that parameter.

According to the probabilistic approach described here, $\bar{I}_m$ can be computed by maximizing, for each mth earthquake, the likelihood function

$$L_m = \sum_{k=1}^{M_m}\ln\left\{\frac{1}{\sigma_m\sqrt{2\pi}}\sum_{I=1}^{12} p_j(I)\int_{I-0.5}^{I+0.5}\exp\left[-\frac{(i-\bar{I}_m)^2}{2\sigma_m^2}\right]di\right\}. \qquad (18)$$

In this way, the average intensity $\bar{I}_m$ and the corresponding S.D. σ_m will be computed for each earthquake to be considered in the analysis. $\bar{I}_m$ can be introduced in equation (16) to compute the value of μ_j to be used in equation (9). The latter equation defines the overall log likelihood to be maximized in order to retrieve the four free parameters (a, b, h, σ).

Second Step

It may be seen, from equation (15), that I_E can be computed easily for all of the well-documented earthquakes, provided that parameters a, b, and h are computed in the first step. This can be achieved by using the relationship

$$I_E = \mu(\bar{I}_m, h) = \bar{I}_m + a(h - \bar{D}_m) + b[\ln(h) - \overline{\ln(D_m)}]. \tag{19}$$

These I_E values can be used, in this second step, to fit empirical regressions with different source parameters (magnitude, I_0, $I_{\max}$), which are generally available for all the earthquakes in the catalog. Such relationships allow I_E to be estimated even for earthquakes that lack a suitable macroseismic data set. As a result, equation (14) (with I_E substituted for J) can be used in place of equation (16) to predict the intensity at a site for all of the earthquakes in the catalog. Of course, a different parameterization of regression uncertainty must be provided in the cases that I_E is obtained directly by the use of equation (19) or is deduced from other epicentral parameters.

Quality and Validation Criteria

Estimation Errors

Under the hypothesis of Normal distribution, errors in estimation can be evaluated from the diagonal terms of the variance–covariance matrix. This matrix can be computed approximately as the inverse of the finite-difference Hessian of the log likelihood $L(\hat{\theta}, \sigma)$ at the maximum (see, i.e., Guo and Ogata, 1997). Since this estimate represents a lower limit, errors are also evaluated by using a numerical resampling procedure (bootstrap). The basic premise of the bootstrap approach (Efron and Tbishirani, 1986; Hall, 1992) is that the empirical frequency distribution of data provides an optimal empirical estimate (in the sense of maximum likelihood) of the probability distribution that characterizes the unknown parent population. This hypothesis implies that any new data sets (usually called bootstrap samples or paradata sets) that are obtained by randomly resampling (with replacements) the original set preserve the statistical features of the parent population. Paradata sets can be used to evaluate (via a distribution-free approach) the sampling properties of a given population parameter from the analysis of the empirical values of the parameter computed from each paradata set. In the present application, several paradata sets were obtained from the original data set. For each paradata set, a new parameterization of the attenuation model was obtained by maximizing the relevant likelihood function (9). In this way, a set of values for the unknown parameters was obtained and may be considered to be representative of the relative parent populations. A distribution-free evaluation of the estimation errors is obtained from these samples by computing the empirical variance–covariance matrix.

Quality Factors

The value of σ obtained from the maximization of L (equation 9) can be considered as a quality parameter to evaluate the fit of the attenuation model to data. Another interesting parameter is the variance explained by the model (R^2), which can be expressed in the form

$$R^2 = \frac{\sigma^2_{\text{ave}} - \sigma^2}{\sigma^2_{\text{ave}}}, \tag{20}$$

where σ_{ave} is the S.D. of the observed intensities with respect to the average value $\bar{I}_m$ for each mth earthquake and is given by

$$\sigma^2_{\text{ave}} = \frac{\sum_{m=1}^{N} \sigma_m^2 M_m}{\sum_{m=1}^{N} M_m}, \tag{21}$$

where N is the number of earthquakes, and σ_m is computed by maximizing equation (18).

Other quality parameters are based on the information theory and are useful for comparing the efficiency of attenuation models with different numbers of degrees of freedom. In what follows, we will consider in particular the Bayesian information criterion (BIC)

$$\text{BIC} = L(\hat{\boldsymbol{\theta}}) - \frac{k}{2} \ln \frac{n}{2\pi} \tag{22}$$

(Schwarz, 1978; Draper, 1995) and the corrected Akaike information criterion (AIC_c)

$$\text{AIC}_\text{c} = L(\hat{\boldsymbol{\theta}}) - k - \frac{k(k+1)}{n-k-1} \tag{23}$$

(Akaike, 1974; Hurvich and Tsai, 1989). In these equations, $\hat{\boldsymbol{\theta}}$ is the set of parameter values maximizing the log-likelihood function $L(\boldsymbol{\theta})$, k is the number of free parameters, and n is the number of independent data used in likelihood maximization. AIC_c and BIC adequately represent the two alternative approaches (frequentist and Bayesian) to information theory in model evaluation. They can be used to compare the efficiency of different models objectively (the higher the value, the better the model) because they consider not only the goodness of fit, but also the number of free parameters. In fact, it is well known that the fit of a model improves when adding further free parameters. However, this does not necessarily imply that the added parameters will significantly improve the predictive ability of the model. In the present analysis, the parameters R^2, BIC and AIC_c were used to compare the performances of alternative formulae for attenuation.

Validation Criteria

Even if the fitting of the attenuation relation is made as good as possible, due to the presence of systematic errors in the data or the inadequacy of the model, the resulting parameterization could fail to represent the data set correctly in the predictive sense. Albarello and D'Amico (2004, 2005) have proposed a validation procedure aimed at testing the overall reliability of the empirical attenuation relationships in their complete probabilistic form. In their approach, the number of observed intensities above given thresholds, for all earthquakes included in the data set, are compared with

those expected on the basis of the considered attenuation model (see Albarello and D'Amico, 2005 for details).

In the previous applications of this test, both the log-linear equation fitted by Albarello and D'Amico (2004) and the bilinear relationship proposed by Gasperini (2001) dramatically failed to pass it. Pasolini *et al.* (2008) showed that the failure was due mostly to incorrect assumptions about the data and the attenuation equation. However, the test still failed even after data sets and equations had been corrected, although the correspondence between predictions and observations improved significantly. The reason for the failure after the corrections is probably that a number of further assumptions implied by the validation procedure (e.g., linearity of the intensity scale, the normality of residual distribution, etc.) are not fully satisfied by the real world. Thus, we do not expect that the deviations between intensities that are observed and predicted by attenuation relationships lie within standard confidence limits for each given intensity threshold. Rather, it is likely that they are reasonably low and symmetrically distributed.

Data Analysis

The two-step procedure described in the section entitled Two-Step Regression Procedure can, in principle, be applied to earthquakes with only a single-intensity observation. However, in order to improve its reliability, we applied it only to earthquakes for which a number of usable observations larger than a minimum threshold $N_{\min}$ is available. Hence, we initially choose only earthquakes with at least $N_{\min} = 10$ remaining intensity data. This further reduces the total number of intensity observations considered for the analysis to 21,932. Following the result shown by Pasolini *et al.* (2008), we also set the maximum distance $R_{\max}$ of sites to be considered in the computation of the average intensities by equation (15) to the maximum epicentral distance (about 300 km). This entails that all the data were considered for such averages. The actual effects of different choices for both $N_{\min}$ and $R_{\max}$ will be analyzed and discussed in the subsequent sections.

Regression Results: First Step

The data set was analyzed following the procedure described previously and using our initial choices for arbitrary parameters ($N_{\min} = 10$, $R_{\min} = 0$, $R_{\max} = \infty$, $w_1 = 0.5$, $w_2 = 0.5$). The maximization of equation (9) with $\mu_j \equiv \mu(\bar{I}_m, D)$ from equation (14) gives $a = (-0.0086 \pm 0.0005)$ deg/km for the coefficient of the linear distance term, $b = (-1.037 \pm 0.027)$ for the coefficient of the natural logarithm of distance, and $h = (3.91 \pm 0.27)$ km for the average depth. Hence, the attenuation equation (14) becomes

$$\mu(I_E, D) = I_E - 0.0086(D - 3.91) - 1.037[\ln(D) - \ln(3.91)], \quad (24)$$

with

$$D = \sqrt{R^2 + 3.91^2}. \quad (25)$$

The corresponding model S.D. is $\sigma = 0.69$, close to the estimate of the intrinsic one determined previously (see section entitled The Data Set). The variance explained by the model (R^2) is 0.656.

The relevant variance–covariance matrix, estimated as the inverse of the numerical Hessian of $L(\hat{\theta}, \sigma)$ at the maximum (standard estimate), is given in Table 2 along with the corresponding bootstrap estimates. The bootstrap estimates were obtained from 1000 paradata sets obtained by random resampling (with replacement) of 21,932 intensity values from the original data set. The comparison between the two matrices indicates that the covariance elements from the Hessian underestimate those provided by the bootstrap analysis by a factor of 20%–30%. This corresponds to an underestimate of parameter errors of the order of 10%–15%.

The presence of a significant multicollinearity is indicated by the analysis of the off-diagonal terms of the variance–covariance matrix. To better demonstrate the mutual covariance between the parameters, the relevant distributions obtained by the bootstrap analysis are shown in Figure 2. We can note a strong inverse correlation between the values of distance coefficients a and b, as well as (slightly lower) between b and h, while the (direct) correlation between a and h is weaker. The high correlation among the parameters indicates that different combinations of their values might result in very similar attenuation equations. The high correlation could also indicate that small differences in the data set will result in apparently strong variations of the empirical parameters, despite the fact that the attenuation patterns are almost indistinguishable.

Table 2
Variance–Covariance Matrix of First-Step Regression

	From Hessian			From Bootstrap			Ratios (H/B)		
	a	*b*	*h*	*a*	*b*	*h*	*a*	*b*	*h*
a	2.35×10^{-7}	-1.19×10^{-5}	8.99×10^{-5}	3.07×10^{-7}	-1.54×10^{-5}	12.2×10^{-5}	0.77	0.77	0.74
b	-1.19×10^{-5}	7.11×10^{-4}	-6.04×10^{-3}	-1.54×10^{-5}	9.23×10^{-4}	-8.25×10^{-3}	0.77	0.77	0.73
h	8.99×10^{-5}	-6.04×10^{-3}	7.31×10^{-2}	1.22×10^{-4}	-8.25×10^{-3}	10.02×10^{-2}	0.74	0.73	0.72

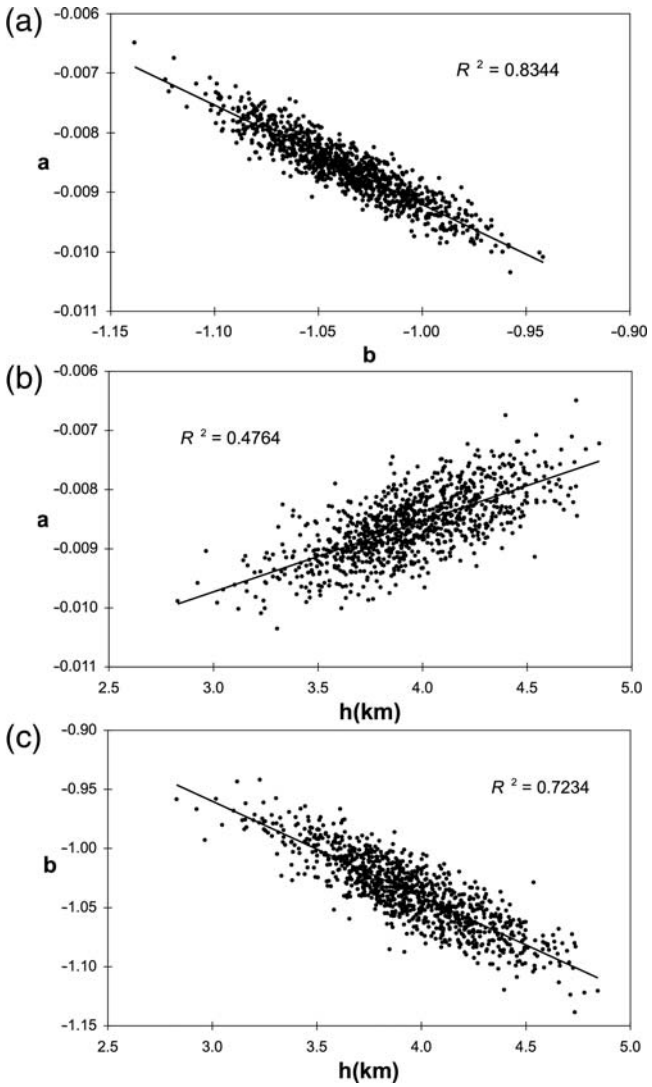

Figure 2. Distribution of parameter values obtained from 1000 bootstrap repetitions. This highlights the high correlation between parameters. The explained variance R^2 is reported in each plot.

Regression Results: Second Steps

For each earthquake in our macroseismic data set, the value of I_E can be computed simply according to equation (19). To compute it for any other earthquake in the catalog, we estimated empirical relations with I_{max}, I_0. The magnitude M_{aw}, which results from combining the instrumental and macroseismic information, was also considered. All three parameters are available for all the earthquakes of the CPTI04 catalog. We also consider for this analysis a reduced set of moment magnitudes M_{sw}, which were either measured directly by moment tensor inversion or deduced from other instrumental magnitudes using empirical conversion rules (Gasperini, 2004).

Figure 3 and Table 3 show the results of ordinary least squares (OLS) and general orthogonal regressions (GOR) of I_E versus I_{max}, I_0, M_{aw}, and M_{sw}. For the GOR, we followed the procedure described by Fuller (1987) and applied by Castellaro *et al.* (2006). In Table 3, the assumed ratios η between the variances of dependent and independent variables for each regression are also reported. To estimate such ratios, which are necessary for applying the GOR method, we assumed that the variances of both I_{max} and I_0 are the square of half a degree (corresponding to the resolution of the macroseismic scale) and that the variance of I_E is 0.0225 (corresponding to the average of the empirical variances computed for each earthquake in our data set). The variances of M_{aw} and M_{sw} (0.0484 and 0.0729, respectively) were computed by averaging the squares of the estimation errors reported in the CPTI04 catalog for each earthquake.

Figure 3a,b shows that the correlation of I_E versus I_0 is slightly better than that versus I_{max}. The regression slopes are very similar, while there is a difference of about half of one degree between the intercepts (Table 3). On average, I_E values result slightly larger than those of I_0 for high intensities and slightly lower than those of I_0 for low ones. In spite of this, there is a substantial coincidence among them, with the average difference being lower than a tenth of a degree. This might appear surprising in the light of the clear discrepancy of about one degree found in the companion article (Pasolini *et al.*, 2008), in which the data sets and the computational frameworks adopted by Albarello and D'Amico (2004) were used. We can explain this different behavior by considering the choices made in the present work concerning the average source depth (estimated from the data and not fixed at 10 km) and the inclusion of near-source data. In fact, if we fix the depth to 10 km and exclude data at distances shorter than 15 km (as was done by Albarello and D'Amico, 2004), the average difference between I_0 and I_E for our data set rises, back to about 0.55 degrees. We may conclude that the marked discrepancy between I_0 and I_E found in the companion article was due mainly to the assumption of an inappropriate source depth and the exclusion of the data in the vicinity of the source.

Concerning the relations involving magnitudes (Fig. 3c, d), we may note in Table 3 a significant difference between the regression slopes for the two magnitudes M_{aw} and M_{sw}. This might appear surprising, given that M_{aw} (which is based both on instrumental and macroseismic information) has been calibrated on essentially the same set of M_{sw} instrumental magnitudes (Gasperini, 2004). However, we may note that such calibration has been made by weighting each instrumental magnitude estimate with the inverse of the respective squared error. This procedure gives higher weights to moment magnitudes computed by the inversion of complete seismograms and lower weights to instrumental magnitudes of the first half of the twentieth century (mainly M_s) computed by maximum amplitudes measured on historical seismograms. The calibration of mechanical instruments used in Italy up to about 1980 is doubtful; hence, we believe that the M_{aw} data set is generally more homogeneous and reliable than the M_{sw}. This implies that M_{aw} values are to be preferred for computing I_E.

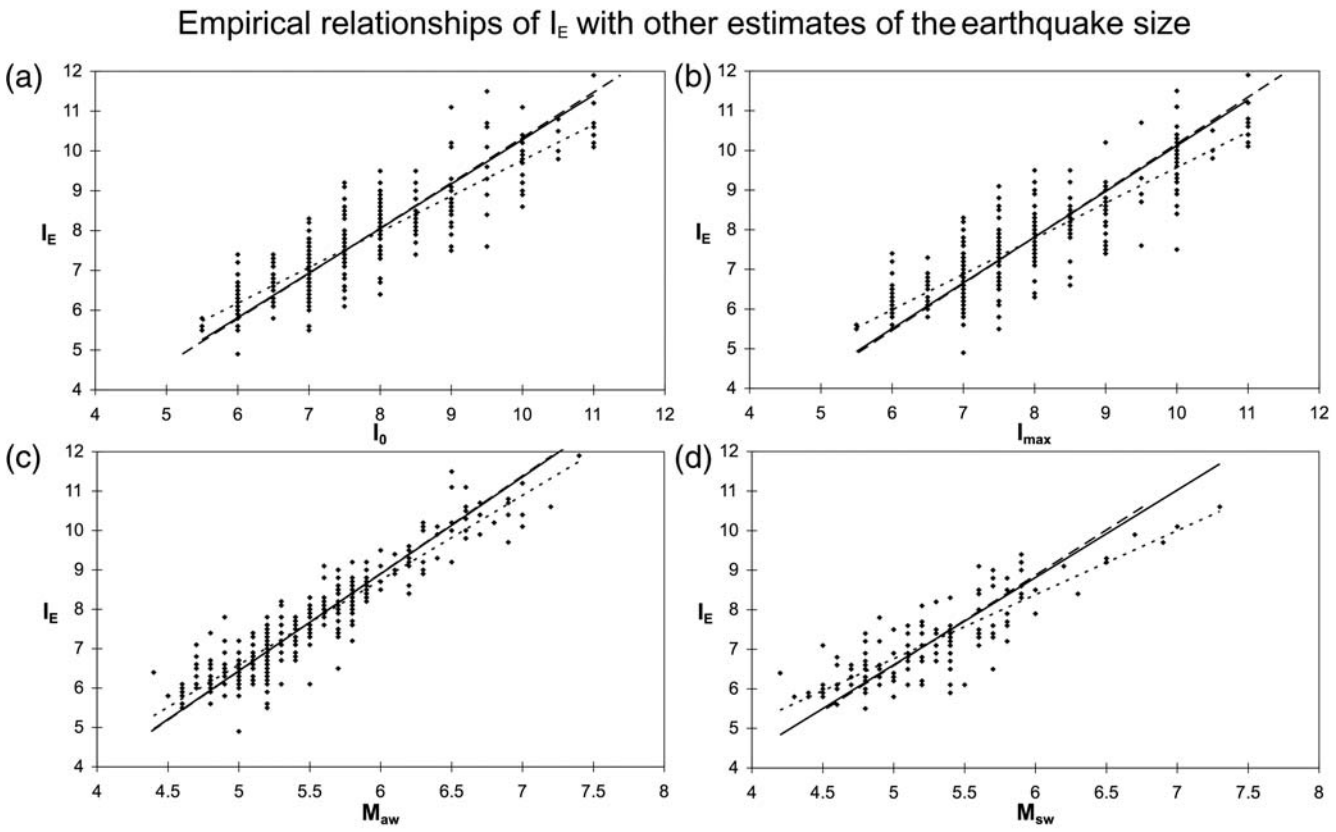

Figure 3. Empirical relations of I_E with I_0, $I_{\max}$, M_{aw} and M_{sw}. Solid lines indicate the result of GOR regression, dotted and dashed lines indicate respectively results of the direct and inverse OLS regressions.

We also tested the alternative choice for computing magnitude coefficients at the same time as the distance terms by an OLS regression of the equation

$$\mu(M, D) = c + dM + a(D - h) + b[\ln(D) - \ln(h)]. \tag{26}$$

Table 4 shows how the values of depth (h) and distance coefficients (a, b) are very close to those deduced from two-step regressions (see previous section), while the magnitude coefficients (c, d) differ significantly from those reported in Table 3 for the OLS method (the results from GOR analysis are not comparable, so they were not considered). We can show that such differences are due to the different weighting of data. In fact, in the two-step regression, all earthquakes have the same weight, while in the regression of equation (26), the weight of each earthquake is proportional to the number of observations. To validate this statement, we performed the regression of I_E versus magnitude using independent estimates of I_E made from individual intensity observations. These can be computed from the equation

$$I_E = I_s - a(D - h) - b \ln\left(\frac{D}{h}\right), \tag{27}$$

where I_s is the individual intensity observed at a distance D from the macroseismic hypocenter located at a depth h and parameters a, b, and h are those of equation (24). The results (Table 5) of OLS regression show values of c and d coefficients close to those found by simultaneous regression. This means that when the data are similarly weighted, two-step and one-step standard regressions give consistent results.

Table 3

Coefficients of Regression of I_E with I_0, $I_{\max}$, M_{aw}, and M_{sw}

Equation	η	c (GOR)	d (GOR)	σ	c (OLS)	d (OLS)	σ
$I_E = c + dI_0$	0.09	-0.893 ± 0.254	1.118 ± 0.033	0.70	0.791 ± 0.444	0.897 ± 0.057	0.63
$I_E = c + dI_{\max}$	0.09	-1.418 ± 0.289	1.154 ± 0.036	0.75	0.591 ± 0.464	0.898 ± 0.058	0.67
$I_E = c + dM_{\mathrm{aw}}$	0.46	-5.862 ± 0.301	2.460 ± 0.055	0.53	-4.157 ± 0.723	2.150 ± 0.131	0.50
$I_E = c + dM_{\mathrm{sw}}$	0.31	-5.230 ± 0.645	2.210 ± 0.122	0.66	-1.343 ± 0.877	1.621 ± 0.166	0.58

From GOR and OLS methods (one observation for each earthquakes). η indicates the assumed variance ratio for each orthogonal regression (see Castellaro *et al.*, 2006).

Table 4

Coefficients for the Simultaneous Regression of Attenuation Coefficients and Magnitudes M_{aw} and M_{sw}

Magnitude	c	d	a	b	h	σ
M_{aw}	-3.062 ± 0.070	1.931 ± 0.010	-0.0126 ± 0.0005	-0.900 ± 0.027	3.696 ± 0.302	0.81
M_{sw}	-1.147 ± 0.096	1.567 ± 0.012	-0.0104 ± 0.0007	-0.912 ± 0.039	4.155 ± 0.511	0.79

As GOR is more appropriate than OLS when the independent variable is affected by errors and a simultaneous GOR of distance and magnitude is not feasible, we believe that the procedure based on a two-step regression for distance and magnitude is preferable to one based on a one-step regression. We also prefer the regression coefficients in Table 3 to those of Table 5 because the former are not biased by the uneven distribution of intensity observations among different earthquakes.

For the earthquakes in the CPTI04 catalog for which the M_{aw} magnitude is simply deduced from I_0 (according to regressions computed by Rebez and Stucchi [1999] and Gasperini [2004]), our preference is to compute I_E directly from the regression with I_0, so avoiding the double conversion from I_0 to M_{aw} and from M_{aw} to I_E.

The total standard errors of separate regressions can be obtained, following the usual error law, by summing the relevant variances of the involved empirical relationships. In the case that I_E is computed (by GOR regression) from I_0 and M_{aw} they are 0.98 and 0.87, respectively (i.e., larger than the value that we computed for the two-step procedure [0.69]).

Discussion and Validation of Regression Results

Sensitivity Analysis

We noted previously that the results of our analysis might also depend on the choices of four arbitrary parameters. In fact, the values of $\bar{D}_m$, $\overline{\ln(D)}_m$, and $\bar{I}_m$, which are used in the first step of the inversion procedure, depend on the value of R_{max} (i.e., the maximum distance from the epicenter of intensity data considered for computing such averages). Moreover, the data of the intensity data set that was actually used for computations were selected on the basis of the values of R_{min} and N_{min} (i.e., the minimum epicentral distance, and the minimum number of intensity data for each event to be considered in the analysis, respectively). Finally, different choices might be made for weights w_1 and w_2 that parameterize uncertainty on intensity data (see the section entitled Statistical Formalization).

In order to quantify the effects of these choices, a sensitivity analysis was performed. In particular, different values of R_{max}, N_{min}, R_{min}, and weights w_1 and w_2 were considered, and for each of them the likelihood function (equation 9) was maximized to obtain different parameterizations of (14). In Figures 4 to 7, variations of model parameters a, b, h, and σ will be shown as a function of different values of the arbitrary parameters R_{max}, N_{min}, R_{min}, and weights w_1 and w_2, respectively.

Figure 4 shows that for an R_{max} larger than 30 km, b and σ are almost insensitive to variations in R_{max}. Parameter a stabilizes when $R_{max} > 50$ and in general shows relatively small sensitivity to R_{max}. A larger sensitivity is shown for h. In particular, h increases monotonically for $R_{max} < 50$ km. Similar results are obtained (Fig. 5) when different choices are considered for parameter N_{min} (set to 10 in the analysis discussed in the previous section). In this case also, h shows the largest sensitivity for $N_{min} < 60$.

In Figure 6, we can see that h also shows the highest variability with respect to R_{min}. In fact, the value of h decreases strongly with increasing R_{min} up to 20 km. This means that the average depth is controlled by the data in the vicinity of the epicenter and that the exclusion of such data makes the depth estimate unrealistic (< 1 km). It is also interesting to note that if the data at distances shorter than 90 km are excluded from computations, the linear term (coefficient a) becomes dominant over the logarithmic one (coefficient b). We may infer that the data in the vicinity of the source, although they are possibly biased by near-source anisotropy for strong events, are still necessary to describe the overall attenuation behavior realistically.

These results indicate that h is the most sensitive to the data selection strategy, particularly with respect to data in the epicentral area. However, it is worth noting that the S.D. of the model is almost unaffected by variations in h.

Figure 7 shows that the regression results are almost insensitive to the choice of the weights w_1 and w_2 that pa-

Table 5

Coefficients of Regression of I_E with I_0, I_{max}, M_{aw}, and M_{sw}

Equation	c (GOR)	d (GOR)	σ	c (OLS)	d (OLS)	σ
$I_E = c + dI_0$	0.068 ± 0.023	0.976 ± 0.003	0.56	1.151 ± 0.055	0.851 ± 0.006	0.53
$I_E = c + dI_{max}$	-0.451 ± 0.026	1.019 ± 0.003	0.59	0.796 ± 0.058	0.878 ± 0.006	0.55
$I_E = c + dM_{aw}$	-3.972 ± 0.028	2.095 ± 0.005	0.45	-2.868 ± 0.082	1.910 ± 0.014	0.44
$I_E = c + dM_{sw}$	-2.129 ± 0.034	1.774 ± 0.006	0.46	-1.055 ± 0.088	1.592 ± 0.015	0.44

From GOR and OLS methods (one observation for each intensity datum).

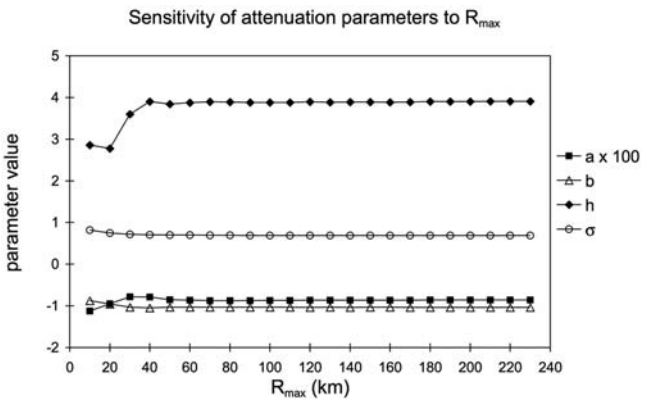

Figure 4. Sensitivity of attenuation parameters to $R_{\max}$ (the maximum epicentral distance of data used in the calculation of $\bar{D}$, $\overline{\ln(D)}$, and $\bar{I}$).

rameterize the probability distribution of uncertain intensity values (see Data Set section). It is interesting to note that even if uncertain data are, following Gasperini (2001), considered simply as representative of real intermediate intensity values (i.e., VII–VIII equal to 7.5) the results (half degrees inset) are affected negligibly and are very similar to those obtained using equal weights ($w_1 = w_2 = 0.5$). This might indicate that uncertain values are probably close to representing ground-motion levels intermediate to those associated to adjacent integer intensities. In addition, the results are very similar (no uncertain degrees inset) except with respect to h, even if the uncertain data are totally ignored in the fit. This similarity indicates a substantial coherence of attenuation properties for uncertain degrees with respect to standard ones.

Validation

Following Albarello and D'Amico (2005), the number of felt intensities above given intensity thresholds were compared (Table 6) with those expected on the basis of the attenuation model (equation 16). The differences between observed and expected values are less than 5% for intensity

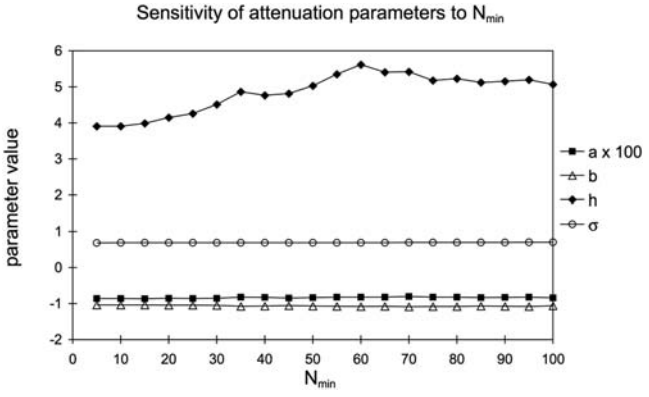

Figure 5. Sensitivity of attenuation parameters to $N_{\min}$ (the minimum number of intensity data for each earthquake included in the fit).

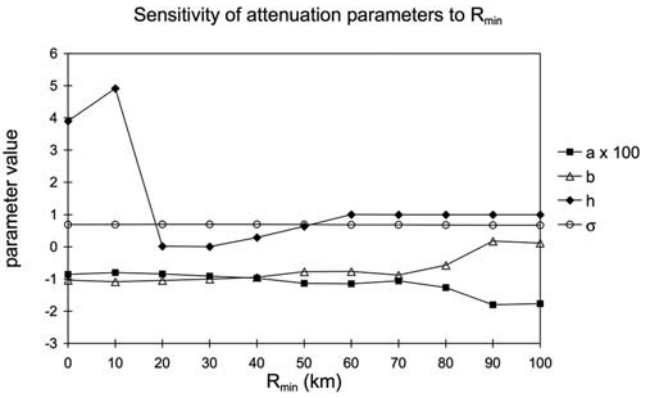

Figure 6. Sensitivity of attenuation parameters to $R_{\min}$ (the minimum epicentral distance of data used for the fit).

thresholds lower than X MCS. For threshold X and XI, the equation (16) model appears to significantly underestimate intensities observed at the sites (overattenuates), while for thresholds VIII and IX, it slightly overestimates observations (underattenuates). The alternate signs of differences between expected and observed numbers of occurrences for various thresholds suggests that such discrepancies might be attributed to a nonlinearity of the relationship between intensity and the logarithm of the ground-motion amplitude.

In particular, the deficiency of real intensity estimates for degree IX with respect to those expected on the basis of the attenuation relationship might indicate that the definitions of such degree in the MCS scale imply ground motion amplitudes larger than those implied by the logarithmic relation with intensity. On the other hand, the underestimation of the occurrences of intensities X and XI might be symptomatic of the possible inadequacy of the model to fit near-source effects of major earthquakes that are responsible for the largest intensities. In fact, the point-source isotropic hypothesis that underlies the results of attenuation model (16) is clearly inadequate to describe the distribution of the largest intensities induced by earthquakes of magnitude larger than 6, whose source length is of the order of tens of kilometers. In these cases, large intensities (> IX) might appear to occur at relatively long distances from the epicenter (the barycenter of their distribution) even though they are actually located very close to the source trace. This implies that the actual occurrences of such strong intensities (that are relatively few) appear to be greater than those expected on the basis of an isotropic relationship that is constrained mainly by the more numerous lower intensities.

Comparison with Alternative Models

As discussed in this article, our choice of the log-linear form of the dependence of intensity with distance is based mainly on its obvious physical justification, but also on its wide use in attenuation studies. However, we also applied the same two-step procedure and the same choices to fit some of the functional relationships so far proposed in the literature.

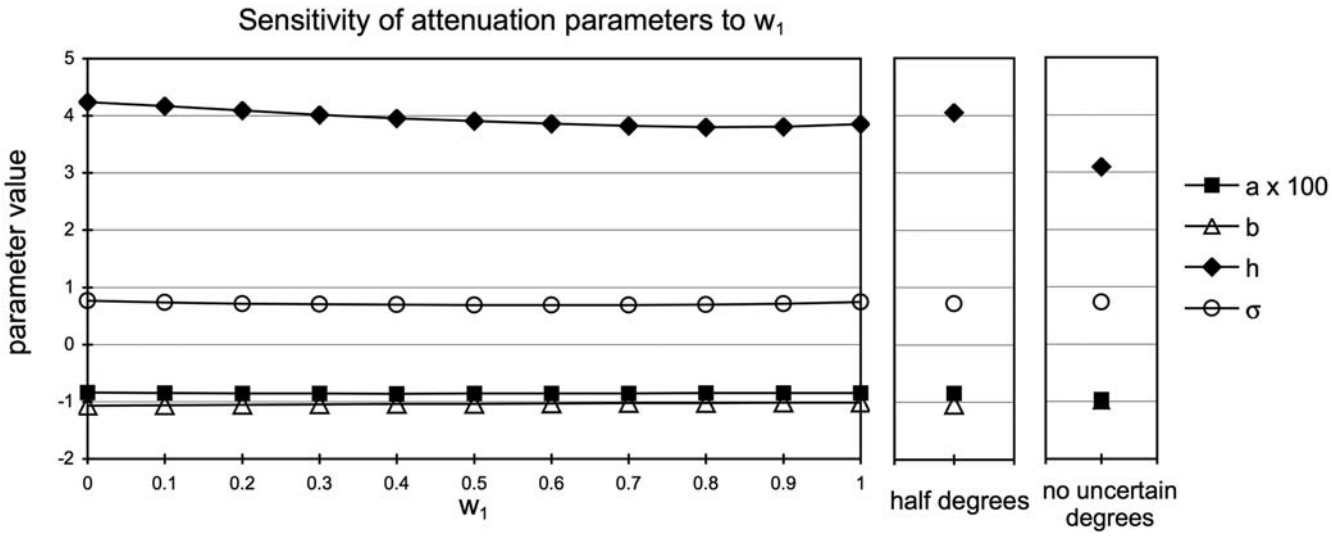

Figure 7. Sensitivity of attenuation parameters by varying the assignment of probabilities for uncertain degrees. w_1 is the probability assigned to the nearer lower degree and $1 - w_1$ is assigned to the nearer higher one. Insets represent parameter values obtained by assigning half-integer intensity values (half degrees) or by discarding all uncertain degrees (no uncertain degrees).

We considered the bilinear model proposed by Gasperini (2001), the cubic root attenuation model (CRAM) proposed by Berardi *et al.* (1993), and a simple logarithmic equation. Note from Table 7 that the log-linear form assumed in this work performs better than any other model previously used to describe intensity attenuation in Italy. The comparison is made on the basis of the before-described statistical and information-based quality factors (σ, R^2, BIC and AIC_c). For all of them, the log-linear model scores better than the bilinear (Gasperini, 2001), the logarithmic, and the cubic root (Berardi *et al.*, 1993) models. This is in tension with the results of a similar comparison made by Gasperini (2001) who, when considering the averages of intensity differences $\Delta I = I_0 - I$ over distance bins of 5 km (and not single-intensity observations), found a clear preference for the bilinear model with respect to the log-linear one. In fact, while such a discrepancy could be attributed to the use of binning, it could also be attributed to the near-source portion of the intensity data set (excluded from computation by Gasperini, 2001) where the logarithmic term, which accounts for geometrical spreading (neglected by Gasperini, 2001), assumes a crucial role. In fact, if a logarithmic term is added to the bilinear model (last line in Table 7), the fit becomes slightly better than the log-linear one. This could confirm the inference made by Gasperini (2001) that anelastic dissipation properties are probably depth dependent. However, the improvement of the fit of the log-bilinear model with respect to the simpler log-linear one is so small that in most cases the complications in hazard computational procedures that its adoption would seem to imply are not justified. For such reasons, we adhere to our choice of the simple log-linear model as the preferred reference attenuation model for hazard assessment.

Table 6

Observed and Predicted Occurrences of Intensities

I	N_{obs}	σ_{obs}	N_{pred}	σ_{pred}	$(1 - N_{pred}/N_{obs})$ %
IV	21,019	10	21,249	23	−1.09
V	18,352	18	18,531	40	−0.98
VI	13,813	17	13,762	45	0.37
VII	9236	22	8814	43	4.57
VIII	4644	20	4663	37	−0.41
IX	1796	14	1856	28	−3.34
X	613	7	503	17	17.94
XI	130	6	87	8	33.08

Observed (N_{obs}) and expected (N_{pred}) number of intensity points above the different thresholds, along with their S.D. (respectively σ_{obs} and σ_{pred}) and percentage difference.

General Discussion and Conclusions

The attenuation pattern of macroseismic intensity in Italy has been analyzed and modeled. The main objective was to develop an attenuation relationship for the probabilistic seismic hazard assessment in Italy in terms of macroseismic intensity. Thus, major attention has been paid to the characterization of the attenuation relationship in its complete probabilistic form. The statistical analysis of intensity was carried out by carefully considering several factors (the discrete character of intensity, uncertainty on original data, completeness, etc.) that have generally been overlooked in previous analyses.

The decision to consider a unique attenuation pattern for the whole Italian area could be considered a basic limitation of the present analysis. We are aware that the peculiar geostructural setting of the Italian peninsula should reflect differentiated attenuation patterns and, in this respect, the attenuation relationship here obtained cannot be considered as a definitive characterization of macroseismic fields in the

Table 7
Comparison between Different Functional Forms of Attenuation Relation

	a	a'	b	h	σ	R^2	BIC	AIC_c
BIL	-0.0591 ± 0.0005	-0.0182 ± 0.0003	—	0.00 ± 0.24	0.7023	0.6435	$-26,105.1$	$-26,097.8$
LOG	—	—	-1.54 ± 0.15	7.77 ± 0.25	0.6943	0.6515	$-25,898.3$	$-25,893.0$
CRAM	-1.2435 ± 0.0076	—	—	1.18 ± 0.22	0.6896	0.6562	$-25,785.0$	$-25,779.8$
LOG LIN	-0.0086 ± 0.0005	—	-1.04 ± 0.27	3.91 ± 0.27	0.6894	0.6565	$-25,781.2$	$-25,773.8$
BIL LOG	-0.0187 ± 0.0026	-0.0108 ± 0.0007	-0.80 ± 0.06	2.78 ± 0.40	0.6891	0.6567	$-25,780.7$	$-25,771.3$

Table is sorted for increasing BIC. The values of AIC_c agree with BIC.

study area. However, the definition of such a reference relationship is a basic preliminary step towards a regionalization of the area under study by using objective quantitative criteria (e.g., Carletti and Gasperini, 2003). A direct consequence of choosing to evaluate an average attenuation pattern is that possible azimuthal or regional variations cannot be considered and thus are neglected.

On the assumption that the general attenuation pattern reflects mainly the seismic energy radiation pattern, the local intensity value has been considered as being dependent on two variables: an expression of the energy radiated at the source and the hypocentral distance (computed assuming a unique hypocentral depth for all the events). The first variable appears to be the most problematic because it is not possible to directly estimate such a parameter from the available documentary data. In the study reported herein, we estimated this parameter from the whole macroseismic field available for each earthquake. In this regard, one should be aware that the number of parameters actually involved in the inversion procedure is much higher than those included explicitly in the attenuation relationship (the coefficients relative to the source strength, the geometrical spreading, the anelastic/scattering dissipation, the average hypocentral depth, and the S.D.) because a source term relative to each of the events has to be included in the computation. In most previous analyses, this role was played by the epicentral intensity I_0, which is usually determined *a priori* by catalog compilers. By contrast, in this work, we introduce a new estimate of radiated energy in terms of the expected intensity at the epicenter I_E for all earthquakes. It is worth noting that although this parameter plays the same formal role in all attenuation equations, it cannot be considered simply as a new estimate of the epicentral intensity I_0, however I_0 is defined. In principle, I_0 should be an integer value, characterized in some cases by an additional uncertainty (e.g., VII–VIII or 7.5), which could be measured directly if a suitable settlement, unaffected by anomalous site amplification, exists at the epicenter. By contrast, the source term introduced here is not constrained to be an integer ordinal value and can be considered as a macroseismic equivalent of magnitude, determined without any direct reference to instrumental parameters. Rather, it is deduced by considering the entire macroseismic field and not from a single or few intensity observations as was done in the case of I_0. That being so, it is less influenced by local site effects or intensity assessment errors. Regression analyses corroborate the feasibility of this interpretation because a satisfactory correlation exists between this energy term and magnitudes. This last result also allows the attenuation relationship here defined to be applied in cases in which knowledge about the relevant macroseismic field is poor, cases that will include earthquakes known only in terms of instrumental parameters. In these cases, I_E can be computed from moment magnitude by using the conversion relationships here determined. Of course, the S.D. relative to intensities estimated by using such a change of variable must be increased appropriately (by the factor here estimated) to take into account the uncertainties of I_E versus moment magnitude relationships.

A stability analysis shows that the resulting attenuation relationship is robust with respect to arbitrary assumptions underlying the modeling approach. In particular, the only parameter seriously affected by these arbitrary choices is the average source depth h, which is (weakly) constrained by the intensity data located in the vicinity of the source only. However, its variability has little influence on the other attenuation parameters and the S.D. of the regression and thus is not relevant for computing seismic hazard. The stability analysis also showed that uncertain intensities (e.g., III–IV) behave similarly to standard intensity estimates and are consistent with semi-integer intensity values (e.g., 3.5). This could justify the use of semi-integer values in simplified approaches.

The ability of the model to predict the actual intensity distribution was also tested by using the procedure proposed by Albarello and D'Amico (2005). Although the best-fitted model failed to pass the test, particularly for intensities higher than VIII, we can reasonably assert that such failure is related to near-source anisotropy and a possible nonlinearity of the intensity scale with respect to ground motion.

The attenuation model determined in this study enables a number of difficulties relative to previous estimates to be overcome (see the companion article by Pasolini *et al.*, 2008). It is almost optimal, because the relevant S.D. is comparable to the intrinsic one related to the scattering of original data (aleatory uncertainty). The intrinsic S.D. is almost independent of the epicentral distance and represents a lower bound for any empirical attenuation relationship that, like the present one, does not consider any regionalization of the area under study, source directionality, or possible local effects. In general, the S.D. associated with the attenuation relationship here yielded results lower than those obtained in previous

works (Gasperini, 2001; Albarello and D'Amico 2004). This could have important consequences in hazard estimates in the Italian region, because the S.D. of the attenuation relationship is well known to affect hazard estimates dramatically (see, e.g., Cornell, 1971; Brillinger, 1982; Albarello and D'Amico, 2004).

The best-fit values and standard errors of attenuation coefficients (-0.0086 ± 0.0005 for the linear term, -1.037 ± 0.027 for the logarithmic one, and 3.91 ± 0.27 for the average depth) suggest some further general considerations:

1. The inferred average source depth is significantly shallower than the average hypocentral depth of strong Italian earthquakes (about 10 km) but quite similar to that (5.0 ± 1.6 km) deduced by the attenuation of PGA in Italy by Sabetta and Pugliese (1987). In their subsequent article, Sabetta and Pugliese (1996) defined such estimate as a fictitious depth determined by the regression, incorporating all of the factors that tend to limit the motion near the source. We could try to explain this discrepancy on the basis of the results of our stability analysis, which demonstrates that the average depth is constrained mainly by the data in the vicinity of the epicenter ($D <$ 20–30 km). We may argue that, for relatively large sources (whose width is of the order of some kilometers), the shallower (and closer) portion of the seismogenic fault contributes more than the deeper one in determining the ground motion level at close sites. This might indicate that the source depth estimated from macroseismic data is likely to reflect a shallower point from which seismic energy appears to be radiated at close sites, rather than the true (and deeper) hypocenter as was hypothesized by past procedures for determining macroseismic depth (von Kővesligethy, 1906; Blake, 1941; Musson, 1996).
2. The value of the linear term coefficient significantly differs from 0 (one order of magnitude larger than the associated standard error). This indicates that the contribution of anelastic dissipation to intensity attenuation is not negligible with respect to geometrical spreading (it becomes of the order of one intensity degree at distances of 100 km).
3. The coefficient of the logarithmic term, close to -1 for the log-linear model and around -0.8 for the log-bilinear model, implies that the geometrical spreading exponent seen by seismic intensity should range from -0.70 to -0.35. These estimates for the geometrical spreading exponent depend on the attenuation model (log linear or log bilinear) and on the assumed coefficient of the linear relation between intensity and the logarithm of PGA, which, for Italy, could vary (in terms of natural logarithms) between the empirical estimate of 0.44 by Margottini *et al.* (1992) and the value of 0.69 assumed by the MCS intensity scale (Cancani, 1904; Sieberg, 1931). This confirms that surface waves (and perhaps reflected and refracted phases), rather than body waves, are likely to have a dominant role to play in determining the seismic intensity observed at a site.

Acknowledgments

We thank Bill Bakun and two anonymous reviewers for their thoughtful comments and suggestions. This work was supported by the Italian Civil Defence Department and the Istituto Nazionale di Geofisica and Vulcanologia (INGV), within the framework of their 2004–2006 Agreement (Project S1). INGV also supported the Ph.D. grant of author C. Pasolini.

References

Akaike, H. (1974). A new look at the statistical model identification, *IEEE Trans. Autom. Control* **19,** 716–723.

Albarello, D., and V. D'Amico (2004). Attenuation relationship of macroseismic intensity in Italy for probabilistic seismic hazard assessment, *Boll. Geofis. Teorica Appl.* **45,** 271–284.

Albarello, D., and V. D'Amico (2005). Validation of intensity attenuation relationships, *Bull. Seismol. Soc. Am.* **95,** 719–724.

Ambraseys, N. N., K. A. Simpson, and J. J. Bommer (1996). Prediction of horizontal response spectra in Europe, *Earthquake Eng. Struct. Dyn.* **25,** 371–400.

Azzaro, R., M. S. Barbano, S. D'Amico, and T. Tuvè (2006). The attenuation of seismic intensity in the Etna region and comparison with other Italian volcanic districts, *Ann. Geophys.* **49,** nos. 4–5, 1003–1020.

Bakun, W. H. (2006). MMI attenuation and historical earthquakes in the basin and range province of western North America, *Bull. Seismol. Soc. Am.* **96,** 2206–2220.

Bakun, W. H., and O. Scotti (2006). Regional intensity attenuation models for France and the estimation of magnitude and location of historical earthquakes, *Geophys. J. Int.* **164,** no. 3596–610.

Bender, B., and D. M. Perkins (1987). *Seisrisk III: a computer program for seismic hazard estimation*, U.S. Geological Survey, Denver, Colorado, 1–48.

Berardi, R., C. Petrungaro, L. Zonetti, L. Magri, and M. Mucciarelli (1993). *Mappe di sismicità per l'area italiana* Istituto Sperimentale Modelli e Strutture (ISMES), Bergamo, Italy, 52 pp. (in Italian).

Blake, A. (1941). On the estimation of focal depth from macroseismic data, *Bull. Seismol. Soc. Am.* **31,** 225–231.

Boschi, E., E. Guidoboni, G. Ferrari, G. Valensise, and P. Gasperini (1995). *Catalogo dei Forti Terremoti in Italia dal 461 a.C. al 1980* Istituto Nazionale di Geofisica/Storia Geofisica Ambiente Srl., Bologna, Italy, 973 pp. (and enclosed CD-ROM; in Italian).

Boschi, E., E. Guidoboni, G. Ferrari, G. Valensise, and P. Gasperini (1997). *Catalogo dei Forti Terremoti in Italia dal 461 a.C. al 1990* Istituto Nazionale di Geofisica/Storia Geofisica Ambiente Srl., Bologna, Italy, 644 pp. (and enclosed CD-ROM; in Italian).

Boschi, E., E. Guidoboni, G. Ferrari, D. Mariotti, G. Valensise, and P. Gasperini (2000). Catalogue of strong Italian earthquakes from 461 B.C. to 1997, *Ann. Geofis.* **43,** 843–868 (and enclosed CD-ROM).

Brillinger, D. R. (1982). Seismic risk assessment: some statistical aspects, *Earthq. Predict. Res.* **1,** 183–195.

Cancani, A. (1904). Sur l'emploi d'une double echelle sismique des intensites, empirique et absolute, *Gerlands Beitr. Geophys., Ergänz.* **2,** 281 (in French).

Carletti, F., and P. Gasperini (2003). Lateral variations of seismic intensity attenuation in Italy, *Geophys. J. Int.* **155,** 839–856.

Carrol, D. L. (1996). Chemical laser modeling with genetic algorithms, *Am. Inst. Aeronaut. Astron.* **34,** 338–346.

Castellaro, S., F. Mulargia, and Y. Y. Kagan (2006). Regression problems for magnitudes, *Geophys. J. Int.* **165,** 913–930.

Chandra, U. (1979). Attenuation of intensities in the United States, *Bull. Seismol. Soc. Am.* **69,** 2003–2024.

Chandra, U., J. G. McWhorter, and A. A. Nowroozi (1979). Attenuation of intensities in Iran, *Bull. Seismol. Soc. Am.* **69,** 237–250.

Cornell, C. A. (1971). Probabilistic analysis of damage to structures under seismic loads, in *Dynamic Waves in Civil Engineering*, D. A. Howells, I. P. Haigh and C. Taylor (Editors), Wiley, New York, 473–493.

Database of Macroseismic Intensity (DBMI) Working Group (2007). *Database macrosismico utilizzato nella compilazione di CPTI04* Istituto Nazionale di Geofisica e Vulcanologia, Milan, available at http://emidius.mi.ingv.it/DBMI04/ (last accessed January 2008; in Italian).

Dennis, J. E., and R. B. Schnabel (1983). *Numerical Methods for Unconstrained Optimization and Nonlinear Equations*, Prentice Hall, New York.

Draper, D. (1995). Assessment and propagation of model uncertainty (with discussion), *J. R. Stat. Soc. Ser. B* **57,** 45–97.

Efron, B., and R. J. Tbishirani (1986). Bootstrap methods for standard errors, confidence intervals and other measures of statistical accuracy, *Stat. Sci.* **1,** 54–77.

Fuller, W. A. (1987). *Measurement Error Models*, Wiley, New York.

Gasperini, P. (2001). The attenuation of seismic intensity in Italy: a bilinear shape indicates dominance of deep phases at epicentral distances longer than 45 km, *Bull. Seismol. Soc. Am.* **91,** 826–841.

Gasperini, P. (2004). Catalogo dei terremoti CPTI2-Appendice 1, in *Redazione della mappa di pericolosità sismica prevista dall'ordinanza PCM del 20 marzo 2003, n. 3274, Rapporto conclusivo*, M. Stucchi (Coordinator), Istituto Nazionale di Geofisica e Vulcanologia, Milan, 29 pp. (also available at http://zonesismiche.mi.ingv.it/documenti/App1.pdf; in Italian).

Gasperini, P., and G. Ferrari (2000). Deriving numerical estimates from descriptive information: the computation of earthquake parameters, *Ann. Geofis.* **43,** 729–746.

Gasperini, P., F. Bernardini, G. Valensise, and E. Boschi (1999). Defining seismogenic sources from historical earthquake felt reports, *Bull. Seismol. Soc. Am.* **89,** 94–110.

Goffe, W., G. D. Ferrier, and J. Rogers (1994). Global optimization of statistical function with simulated annealing, *J. Econom.* **60,** 65–99.

Goldberg, D. E. (1989). *Genetic Algorithms in Search, Optimization and Machine Learning*, Addison–Wesley, Reading, Massachusetts, 77 pp, Chapters 1 and 4, 106–122.

Grünthal, G. (1998). European macroseismic scale 1998, *Cah. Cent. Eur. Géodyn. Séism.* **13,** 1–99.

Guo, Z., and Y. Ogata (1997). Statistical relations between the parameters of aftershock in time, space and magnitude, *J. Geophys. Res.* **102,** 2857–2873.

Gupta, I. N., and O. W. Nuttli (1976). Spatial attenuation of intensities for central U.S. earthquakes, *Bull. Seismol. Soc. Am.* **66,** 743–751.

Hall, P. (1992). *The Bootstrap and Edgeworth Expansion*, Springer, New York.

Holland, J. H. (1975). *Adaptation in Natural and Artificial Systems*, MIT Press, Cambridge, Massachusetts.

Howell, B. F., and T. T. Schultz (1975). Attenuation of modified Mercalli intensity with distance from the epicenter, *Bull. Seismol. Soc. Am.* **65,** 651–665.

Hurvich, C. M., and C.-L. Tsai (1989). Regression and time series model selection in small samples, *Biometrika* **76,** 297–307.

Lee, K., and J. Kim (2002). Intensity attenuation in the Sino-Korean craton, *Bull. Seismol. Soc. Am.* **92,** 783–793.

Magri, L., M. Mucciarelli, and D. Albarello (1994). Estimates of site seismicity rates using ill-defined macroseismic data, *Pure Appl. Geophys.* **143,** 617–632.

Margottini, D., D. Molin, and L. Serva (1992). Intensity versus ground motion: a new approach using Italian data, *Eng. Geol.* **33,** 45–58.

McGuire, R. K. (Editor) (1993). *The Practice of Earthquake Hazard Assessment*, Int. Assoc. Seism. Phys. Earth's Interior, Denver, Colorado, 1–284.

Metropolis, N., and S. M. Ulam (1949). The Monte Carlo method, *J. Am. Stat. Assoc.* **44,** 335–341.

Monachesi, G., and M. Stucchi (1997). GNDT Open-File Rept. DOM4.1, Un database di osservazioni macrosismiche di terremoti di area italiana al di sopra della soglia del danno, Gruppo Nazionale per la Difesa dai Terremoti (GNDT), Milano-Macerata, http://emidius.mi.ingv.it/DOM/home.html (last accessed January 2008; in Italian).

Musson, R. M. V. (1996). Determination of parameters for historical British earthquakes, *Ann. Geofis.* **39,** 1041–1047.

Musson, R. M. V. (2005). Intensity attenuation in the UK, *J. Seism.* **9,** no. 1, 73–86.

Parametric Catalog of Italian Earthquakes (CPTI) Working Group (2004). *Catalogo Parametrico dei Terremoti Italiani (CPTI04)* Istituto Nazionale di Geofisica e Vulcanologia, Milan, available at http://emidius.mi.ingv.it/CPTI04/ (last accessed January 2008; in Italian).

Pasolini, C., P. Gasperini, D. Albarello, B. Lolli, and V. D'Amico (2008). The attenuation of seismic intensity in Italy, part I: Theoretical and empirical backgrounds, *Bull. Seismol. Soc. Am.* **98,** no. 2, 682–691.

Peruzza, L. (1996). Attenuating intensities, *Ann. Geofis.* **34,** 1079–1093.

Rebez, A., and M. Stucchi (1999). Determinazione dei coefficienti della relazione tabellare $I_o - M_s$, in *Catalogo Parametrico dei Terremoti Italiani* Editrice Compositori, Bologna, 20–21 (in Italian).

Rotondi, R., and G. Zonno (2004). Bayesian analysis of a probability distribution for local intensity attenuation, *Ann. Geophys.* **47,** 1521–1540.

Sabetta, F., and A. Pugliese (1987). Attenuation of peak horizontal acceleration and velocity from Italian strong-motion records, *Bull. Seismol. Soc. Am.* **77,** 1491–1513.

Sabetta, F., and A. Pugliese (1996). Estimation of response spectra and simulation of nonstationary earthquake ground motions, *Bull. Seismol. Soc. Am.* **86,** 337–352.

Schwarz, G. (1978). Estimating the dimension of a model, *Ann. Stat.* **6,** 461–464.

Sieberg, A. (1931). Erdebeben, in *Handbuch der Geophysik*, B. Gutenberg (Editor), Vol. **4**, 552–554 (in German).

Tilford, N. R., U. Chandra, D. C. Amick, R. Moran, and F. Snider (1985). Attenuation of intensities and effect of local site conditions on observed intensities during the Corinth, Greece, earthquakes of 24 and 25 February and 4 March 1981, *Bull. Seismol. Soc. Am.* **75,** 923–937.

Visual Numerics (1997). *International Mathematics and Statistics Library (IMSL) Volumes l and 2* Visual Numerics Inc., Houston.

von Kővesligethy, R. (1906). Seismonomia, *Boll. Soc. Sismol. Italy* **11,** 113–250 (in Latin).

Wells, D. L., and K. J. Coppersmith (1994). New empirical relationships among magnitude, rupture length, rupture width, rupture area and surface displacement, *Bull. Seismol. Soc. Am.* **84,** 974–1002.

Dipartimento di Fisica
Università di Bologna
Viale Berti Pichat 8
I-40127 Bologna, Italy
chiara.pasolini@gmail.com
paolo.gasperini@unibo.it
barbara.lolli@unibo.it
(C.P., P.G., B.L.)

Dipartimento di Scienze della Terra
Università di Siena
Via Laterina 8
I-53100 Siena, Italy
albarello@unisi.it
(D.A., V.D.)

Manuscript received 2 February 2007